processes

MDPI

Article

Atomic Orbital Search Algorithm for Efficient Maximum Power Point Tracking in Partially Shaded Solar PV Systems

Md Tahmid Hussain [1], Mohd Tariq [1,*], Adil Sarwar [1], Shabana Urooj [2,*], Amal BaQais [3] and Md. Alamgir Hossain [4]

[1] Department of Electrical Engineering, ZHCET, Aligarh Muslim University, Aligarh 202002, India; gk3910@myamu.ac.in (M.T.H.); adil.sarwar@zhcet.ac.in (A.S.)
[2] Department of Electrical Engineering, College of Engineering, Princess Nourah bint Abdulrahman University, P.O. Box 84428, Riyadh 11671, Saudi Arabia
[3] Department of Chemistry, College of Science, Princess Nourah bint Abdulrahman University, P.O. Box 84428, Riyadh 11671, Saudi Arabia; aabaqeis@pnu.edu.sa
[4] Queensland Micro and Nanotechnology Centre, Griffith University, Nathan, QLD 4111, Australia; mdalamgir.hossain@griffith.edu.au
* Correspondence: tariq.ee@zhcet.ac.in (M.T.); smurooj@pnu.edu.sa (S.U.)

Abstract: The efficient extraction of solar PV power is crucial to maximize utilization, even in rapidly changing environmental conditions. The increasing energy demands highlight the importance of solar photovoltaic (PV) systems for cost-effective energy production. However, traditional PV systems with bypass diodes at their output terminals often produce multiple power peaks, leading to significant power losses if the optimal combination of voltage and current is not achieved. To address this issue, algorithms capable of finding the highest value of a function are employed. Since the PV power output is a complex function with multiple local maximum power points (LMPPs), conventional algorithms struggle to handle partial shading conditions (PSC). As a result, nature-inspired algorithms, also known as metaheuristic algorithms, are used to maximize the power output of solar PV arrays. In this study, we introduced a novel metaheuristic algorithm called atomic orbital search for maximum power point tracking (MPPT) under PSC. The primary motivation behind this research is to enhance the efficiency and effectiveness of MPPT techniques in challenging scenarios. The proposed algorithm offers several advantages, including higher efficiency, shorter tracking time, reduced output variations, and improved duty ratios, resulting in faster convergence to the maximum power point (MPP). To evaluate the algorithm's performance, we conducted extensive experiments using Typhoon HIL and compared it with other existing algorithms commonly employed for MPPT. The results clearly demonstrated that the proposed atomic orbital search algorithm outperformed the alternatives in terms of rapid convergence and efficient MPP tracking, particularly for complex shading patterns. This makes it a suitable choice for developing an MPP tracker applicable in various settings, such as industrial, commercial, and residential applications. In conclusion, our research addresses the pressing need for effective MPPT methods in solar PV systems operating under challenging conditions. The atomic orbital search algorithm showcases its potential in significantly improving the efficiency and performance of MPPT, ultimately contributing to the optimization of solar energy extraction and utilization.

Keywords: atomic orbital search (AOS); maximum power point tracking (MPPT); metaheuristic algorithms; partial shading condition (PSC); photovoltaic (PV)

Citation: Hussain, M.T.; Tariq, M.; Sarwar, A.; Urooj, S.; BaQais, A.; Hossain, M.A. Atomic Orbital Search Algorithm for Efficient Maximum Power Point Tracking in Partially Shaded Solar PV Systems. *Processes* **2023**, *11*, 2776. https://doi.org/10.3390/pr11092776

Academic Editors: Ambra Giovannelli and Mohan Lal Kolhe

Received: 19 July 2023
Revised: 31 August 2023
Accepted: 11 September 2023
Published: 17 September 2023

1. Introduction

Pollution from coal-based energy generation systems poses a grave health and climate hazard to the entire planet. Adopting renewable energy sources to meet the growing energy demand is a viable solution [1], and dedicated steps to harness energy from renewable energy sources with extensive research are the need of the hour. Energy has been the focal

point of discussion in almost all renewable energy programs across the globe. Research has mainly focused on developing efficient technology to convert the energy from sunlight into something useful, such as electricity. Sunlight can be converted to electricity in the following two ways:

1. Thermal energy of sunlight into electrical energy;
2. Direct conversion of sunlight to DC electricity by solar PV.

Research has also been focused on efficient algorithms that can help extract maximum power from solar PV-based energy generation systems. The present work refers to developing an efficient algorithm that can track and obtain maximum power from a solar PV-based electricity generation system.

1.1. Solar PV Array

A solar PV array is a collection of interconnected solar panels, each comprising multiple photovoltaic cells, designed to capture sunlight and convert it directly into electricity through the photovoltaic effect. These arrays are strategically configured to optimize solar exposure and energy capture, forming a functional unit capable of generating electrical power from the sun's radiant energy. The power output is insignificant from a single PV cell. Ten multiple cells are connected in series to form a solar panel with a much higher voltage and power rating. The panels are further connected in a series or parallel fashion, which is shown in Figure 1, to obtain a higher voltage and current, thereby increasing the power rating required for the application. The number of panels can go up to thousands for large PV plants that can feed power to the grid. Solar PV arrays are used for various applications, ranging from small-scale residential installations to large-scale commercial and utility-level solar farms, contributing to the generation of clean and renewable energy [2].

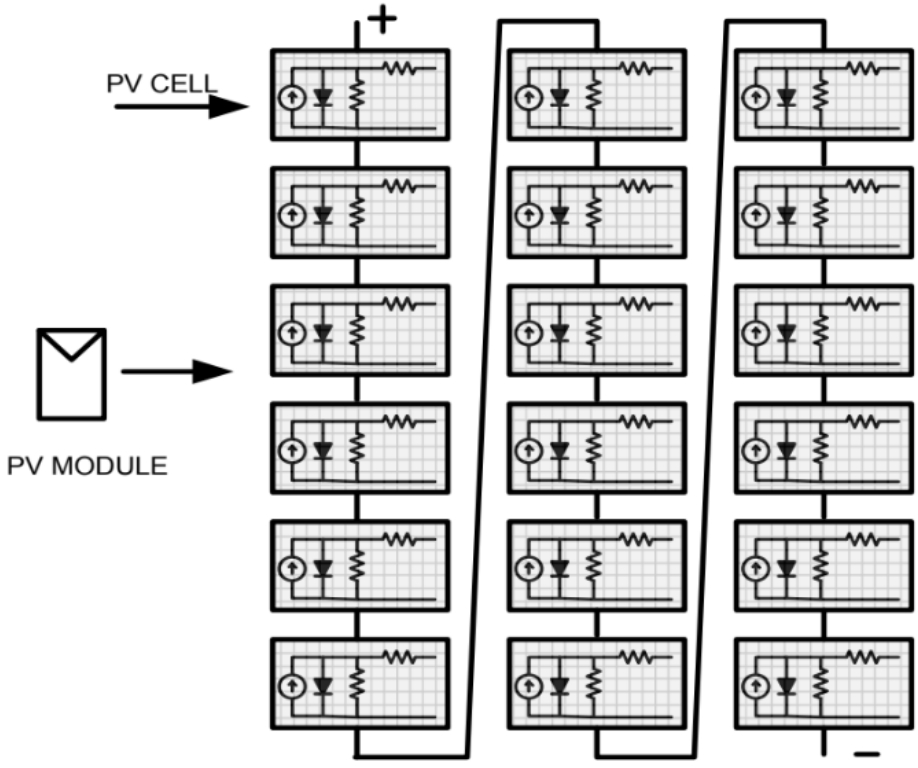

Figure 1. Formation of Solar PV module from the series connection of solar PV cells.

1.2. Non Linear IV Characteristics

The major issue associated with solar PV output utilization is the nonlinear IV and PV characteristics of the solar PV panel [3]. Figures 2 and 3 show, respectively, the current-

versus-voltage and power-versus-voltage curve graph of a PV module during PSC. The reverse bias effect caused by PS on a two-module system is shown in Figure 2.

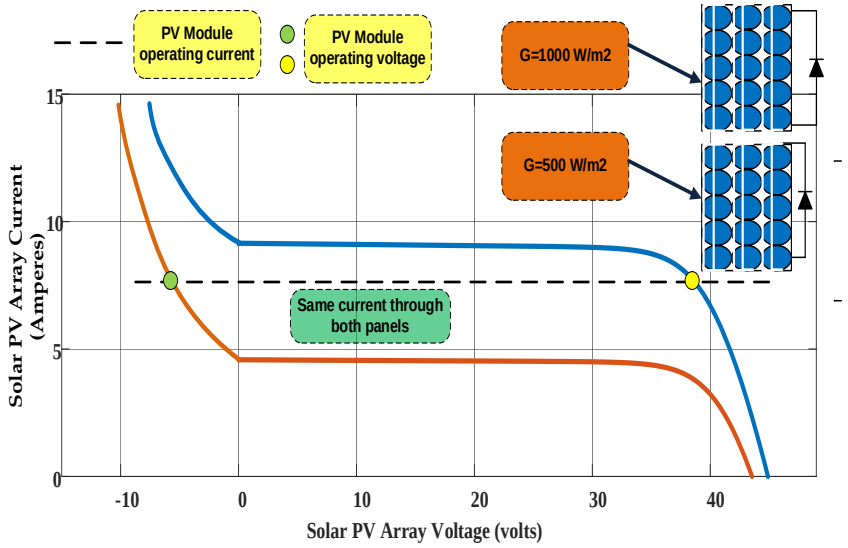

Figure 2. IV characteristic curve with PSC.

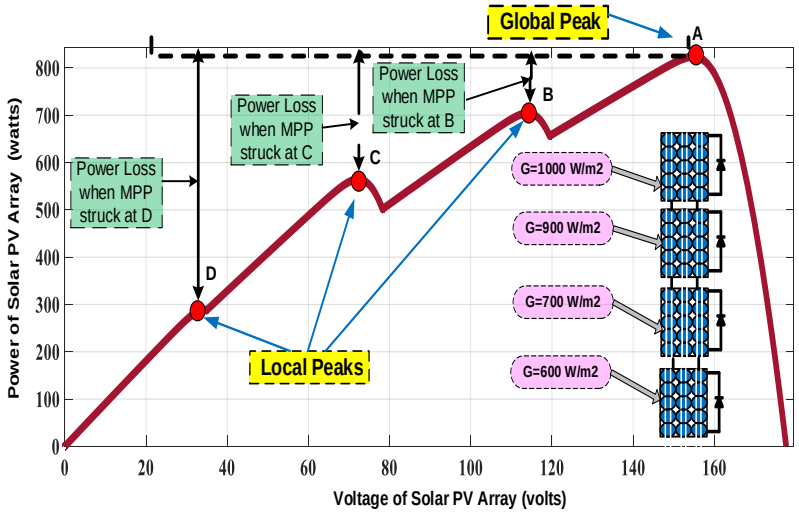

Figure 3. PV characteristics curve with PSC.

Figure 2 shows the two IV characteristic curves of a solar panel with partial shading of 1000 m/s^2 and 500 m/s^2. The IV characteristic shows how the current flows through the solar panel as the voltage increases. The blue line represents the IV curve at an irradiance value of 1000 m/s^2, whereas the red line presents the IV curve at an irradiance value of 500 m/s^2. The current is proportional to the voltage, up to a point. Beyond that point, the current starts to saturate and does not increase as much with increasing voltage. The saturation point is the point at which the solar panel produces the maximum amount of power, and the maximum power point is the point on the IV curve where the power is the greatest. The current output of the panel decreases as the level of shading increases, whereas the voltage output of the panel remains constant as the level of shading increases. Furthermore, the IV curve shifts to the right as the level of shading increases. This means that the panel requires a higher voltage to reach the same current output.

The breakdown voltage, also referred to as the reverse breakdown voltage, signifies the point at which a semiconductor device, such as a PV cell/module, experiences a sudden surge in current when reverse-biased. This phenomenon, often associated with

'avalanche breakdown' or 'Zener breakdown', emerges due to the intense electric field in the semiconductor depletion region, which results in the release of charge carriers through collision processes, leading to a rapid increase in current. Furthermore, bias voltage, encompassing both forward and reverse bias conditions, plays a pivotal role in the operation of PV cells/modules. When reverse bias is applied—by introducing a negative voltage to the cell's terminals—it can unintentionally occur due to factors such as shading or night-time operation. It is paramount to recognize that this reverse-bias operation can trigger unintended adverse effects, including potential damage to the cell/module due to excessive current during the breakdown phase.

Figure 3 shows the IV characteristic curve of a solar panel with partial shading. The current-voltage (IV) curve of a solar PV array provides valuable insights into its behavior under varying conditions, including partial shading. Under normal, unshaded conditions, the IV curve depicts a characteristic shape where the current increases linearly with voltage until it reaches a peak known as the maximum power point (MPP). However, under partial shading, this curve can exhibit unique characteristics due to non-uniform illumination across the array, which can be seen in Figure 3.

When partial shading occurs on a PV array, the IV curve can exhibit multiple local MPPs. These are points where a shaded portion of the array operates at its peak power output considering its specific current-voltage relationship. Each shaded section of the array will have its own local MPP, and the overall power generation can be limited to the lowest of these local MPPs. This limitation arises because the shaded sections act as resistors, causing voltage drops and reducing the current flow. As a result, the local MPPs represent the optimal operating points for each shaded area, whereas the global MPP represents the point on the IV curve where the entire array operates at its maximum power output. It considers the collective effect of all shaded and unshaded sections of the array. Achieving the global MPP is a challenge under partial shading, as the voltage and current variations due to shading can push the system away from this optimal point. Strategies such as bypass diodes, shading analysis, and advanced MPPT algorithms aim to guide the system towards the global MPP by dynamically adjusting the current-voltage characteristics of the array. The PV module power output also decreases directly with shading. However, shading has no impact on the PV module efficiency or fill factor [4]. The maximum power available at a unique knee point needs to be tracked under insulated conditions. Solar panels connected in a series receive different irradiance due to shading from the passing clouds. This leads to a hotspot formation problem, which may lead to failure of the PV panel because of the rise in temperature of the shaded panel. The bypass diodes can mitigate the problem [5]. Bypass diodes are connected in parallel to each panel. The shaded panel is bypassed during shading, avoiding hotspot formation.

As a result, the MPPT becomes more difficult since conventional algorithms, including those focused on hill climbing, involve iteratively increasing or decreasing the input voltage or current until the MPP is reached. However, with nonlinear IV and PV characteristics, the MPP can be a local peak, and hill climbing algorithms can get stuck at this peak and not reach the global MPP. This can result in power losses.

Modifications to the panel array may be built to employ bypass diodes, module level power electronics, or microinverters to prevent these losses. Furthermore, there are a number of MPPT algorithms that have been developed to address the challenges of nonlinear IV and PV characteristics. These algorithms typically use more sophisticated techniques than hill climbing, such as genetic algorithms (GA), particle swarm optimization (PSO), and artificial neural networks (ANN). These algorithms are able to track the MPP more accurately and efficiently, which can lead to improved power output and reduced power losses.

There are several methods proposed for MPPT, which can be broadly classified into two categories: open-loop and closed-loop methods. Open-loop methods do not require any measurement of the PV module or array current or voltage, while closed-loop methods require the measurement of the PV module or array current and voltage. Open-loop

methods are simple and easy to implement, but they are also affected by environmental conditions and the PV module or array characteristics. Closed-loop methods are more accurate and efficient, but they also require more complex hardware and control algorithms.

A comparison table contrasting open-loop and closed-loop methods for MPPT is shown in Table 1. This table highlights key differences between open-loop and closed-loop methods for MPPT, emphasizing aspects such as measurement requirements, implementation complexity, accuracy, efficiency, hardware, and adaptability. It provides a quick overview to help understand the pros and cons of each approach in the context of MPPT techniques.

Table 1. Comparison between open-loop and closed-loop methods for MPPT.

Aspect	Open-Loop Methods	Closed-Loop Methods
Measurement Requirement	No measurement of PV module/array current or voltage is needed.	Requires measurement of PV module/array current and voltage.
Simplicity of Implementation	Simple and easy to implement, suitable for basic setups.	More complex in implementation due to measurement and control requirements.
Environmental Impact	Susceptible to environmental conditions, leading to potentially reduced accuracy.	Less influenced by environmental factors, offering higher accuracy.
PV Module/Array Impact	Affected by PV module/array characteristics, which can lead to suboptimal performance.	More accurate adaptation to PV module/array characteristics, leading to better performance.
Efficiency	Typically less efficient due to limited adjustment accuracy.	Generally more efficient, as they can fine-tune adjustments.
Hardware Complexity	Requires simpler hardware compared to closed-loop methods.	Requires more complex hardware due to measurement and feedback components.
Control Algorithms	Simpler control algorithms are used for basic voltage or power adjustments.	More sophisticated control algorithms are needed for precise adjustments.
Adaptability	May struggle with dynamic changes or partial shading scenarios.	Better adaptability to changing conditions and shading scenarios.
Applications	Suited for smaller, cost-sensitive setups with minimal hardware requirements.	Ideal for larger installations or scenarios requiring higher accuracy and performance.

Recently, several metaheuristic algorithms have been proposed for MPPT. Metaheuristic algorithms are optimization techniques inspired by natural processes, such as genetic algorithms (GA), particle swarm optimization (PSO), and ant colony optimization (ACO). These algorithms have demonstrated their effectiveness in solving complex and nonlinear optimization problems, including MPPT, as compared to the conventional algorithm such as "Perturb and Observe" (P&O). This method involves perturbing the operating point of the photovoltaic system and observing the resulting change in power output to determine the direction to adjust the operating point for the MPP. In one case, the conventional algorithm tracked the MPP, while for the other case it failed [6,7]. The conventional algorithm, though simple and efficient in tracking the optimal value, failed when employed for tracking power under PSC. After their failure, artificial intelligence (AI)-based algorithms, such as fuzzy logic control (FLC) [8], artificial neural network (ANN) [9,10], etc., were employed. The algorithms were proven successful in tracking the maximum power under partially shaded conditions, but the training that they required posed a huge burden on the computer's memory. Hence, finally, the nature-inspired algorithms that were employed.

The work presented in [11] provides a thorough comparative analysis between classical and metaheuristic MPPT algorithms, specifically focusing on PV systems operating under uniform conditions. By examining the merits and limitations of various optimization strategies, the study offers valuable insights into the performance and adaptability of MPPT algorithms in scenarios where shading effects are uniform and, similarly, the significance

of incorporating a comprehensive range of metaheuristic optimization algorithms. One notable contribution in this domain is in [12], which introduces a classification of evolutionary optimization methods into nine distinct categories.

The genetic algorithm (GA) is a search algorithm that is inspired by the processes of natural selection and evolution. GA can be used to find the global optimum of a function by simulating the processes of reproduction, mutation, and selection [13]. GA has been shown to be effective for MPPT, especially for PV systems with non-linear and complex characteristics [14]. Another popular metaheuristic algorithm for MPPT is particle swarm optimization (PSO). PSO is a search algorithm that is inspired by the behavior of a group of birds or fish searching for food. PSO can be used to find the global optimum of a function by simulating the processes of cooperation, competition, and adaptation [15]. PSO has been shown to be effective for MPPT, especially for PV systems with changing environmental conditions [16,17].

The work presented in [18] offers an examination of the validation process for the recently developed jellyfish search optimization (JSO) algorithm. It focuses on its application to the challenge of maximum power point tracking in solar photovoltaic (PV) systems under conditions of partial shading. The JSO algorithm, inspired by the foraging behavior of jellyfish in the ocean, operates as a swarm-insight-driven method [19]. The study in [18] presents a comprehensive exploration of the operational principles underlying the JSO strategy, visually illustrating its key operational steps. Furthermore, a simulation was conducted to assess the performance of the JSO algorithm across diverse scenarios, including static and dynamic irradiance conditions within the PV system. Moreover, the study in [20] offers a significant contribution to this discourse. This study conducted an insightful economic analysis focused on the influence of shading effects from transmission lines on investment decisions concerning photovoltaic power plants. The case study approach employed provides valuable insights into the financial considerations and implications of shading phenomena in solar energy systems. Ant colony optimization (ACO) is another metaheuristic algorithm that has been proposed for MPPT. ACO is a search algorithm that is inspired by the behavior of ants searching for food. ACO can be used to find the global optimum of a function by simulating the processes of communication, cooperation, and adaptation [21]. ACO has been shown to be effective for MPPT, especially for PV systems with changing environmental conditions and non-linear characteristics [22]. Similarly, other various nature-inspired algorithms have been used in the literature to obtain the maximum power out of a solar PV array, such as the Jaya algorithm [23], gravitational search algorithm (GSA) [24], teaching learning-based optimization (TLBO) algorithm [25], coyote optimization algorithm (COA) [26], a very commonly used PSO algorithm with various modifications [27,28], adaptive radial movement optimization (ARMO) algorithm [29], etc. These algorithms, due to their search space exploration capability that is exploited to find the optimal solution, were found very useful for MPPT applications. Their exploration property does not let them get stuck on local maxima. Moreover, they require no huge data feeds in their learning process, unlike AI-based algorithms. These algorithms differ in their performances on the basis of various parameters, such as tracking time, tracking efficiency, output fluctuations, etc.

In recent years, several hybrid metaheuristic algorithms have been proposed for MPPT that combine the advantages of different metaheuristic algorithms. For instance, a hybrid of PSO and GA, called PSOGA, has been proposed for MPPT [30], which takes the advantages of both methods by combining the exploration capability of GA with the exploitation capability of PSO. Another hybrid metaheuristic algorithm called Cuckoo Search-Particle Swarm Optimization (CS-PSO) was proposed for MPPT [31], which combines the global search capability of Cuckoo Search with the local search capability of PSO. Likewise, there are several other recently proposed hybrid metaheuristic algorithms that have been used for MPPT under PSC, such as Cat Swarm Optimization (CSO) with Firefly Algorithm (FF) [32], tunicate swarm algorithm (TSA) with the particle swarm optimization (PSO) [33], Spotted Hyena and Quadratic Approximation [34], Harris Hawk Optimization

(HHO) and P&O [35], P&O using a simulated annealing (SA) algorithm [36], Particle-Swarm-Optimization-Trained Machine Learning and Flying Squirrel Search Optimization (FSSO) [37], etc. Furthermore, these hybrid metaheuristic algorithms have shown better performance in terms of convergence speed, accuracy, and robustness compared to their individual counterparts.

Main contribution of the paper:

(a) Introduction of a New Metaheuristic Algorithm: This paper presents a novel and efficient metaheuristic algorithm AOS for MPPT in solar photovoltaic systems. The algorithm details are comprehensively explained, emphasizing its unique characteristics that make it suitable for MPPT applications.

(b) Real-Time Results Using Typhoon HIL: The proposed algorithm real-time results were obtained using a Typhoon Hardware-in-the-Loop (HIL) simulation. This showcased the practical applicability and effectiveness of the algorithm in a simulated real-world environment.

(c) Comparison with Nature-Inspired Algorithms: This study went beyond introducing the new algorithm by comparing its performance against three well-established nature-inspired algorithms: Phasor-PSO, Cuckoo Search, and Jaya. These comparisons were carried out using Typhoon HIL under varying shading conditions, demonstrating the superiority of the proposed algorithm.

(d) Robustness Under Varying Weather Conditions: This paper validated the robustness and performance of the proposed algorithm under diverse PS scenarios, where peak power points were situated at different positions. This demonstrates the algorithm's adaptability to varying weather conditions and shading patterns.

(e) Superior Performance Metrics: The findings from the comparisons indicate that the novel technique outperformed existing algorithms in several key aspects:

- Faster Convergence: The proposed algorithm required less time to converge to the maximum power point.
- Convergence Value: It achieved higher convergence values to the maximum power output.
- Reduced Power Fluctuations: The proposed algorithm led to smaller fluctuations in power output.
- Frequency of Power Fluctuations: The frequency of power fluctuations was lower, indicating better stability.
- Better Efficiency in Tracking MPP: The proposed algorithm achieved better efficiency of tracking MPP compared to recently proposed metaheuristic algorithms.

(f) Key Characteristics of the Proposed MPPT Method: One of the significant contributions of this study was the development of an MPPT method with specific advantages:

- Low Computing Cost: The proposed algorithm is computationally efficient.
- Robustness: It demonstrated robustness against varying insolation conditions.
- Rapid Convergence: The algorithm achieved quick convergence to the maximum power point.
- No Dependency on Random Number Generation: Unlike certain algorithms, it does not rely heavily on random number generation.
- Negligible Power Oscillations: The algorithm resulted in minimal power oscillations.

The sections are grouped into the following groups: Section 2 discusses the impact of partial shading (PS) on a PV module. Section 3 provides a detailed explanation of the proposed algorithm, AOS, and its workings. Section 4 describes the implementation of AOS for MPPT. Section 5 discusses the experimental findings of the proposed algorithm and compares them to state-of-the-art algorithms, such as Jaya, Phasor-PSO, and Cuckoo search. Section 6 concludes the paper.

2. Partial Shading on Solar PV Array

Partial shading occurs when a solar photovoltaic (PV) array is subjected to varying levels of shading due to factors such as nearby structures, trees, clouds, or dust. The varying levels of shading occur when the sun's rays are blocked from making contact with the surface of a solar photovoltaic cell when the cell is partially shaded by an object, such as a structure, a tree limb, bird droppings, or any other similar object. In a PV array, solar panels are interconnected in series and parallel configurations to harness sunlight and convert it into electricity. However, when shading falls on one or more panels, it can significantly impact the overall performance of the array, leading to reduced power output and efficiency. Figure 4 depicts a Single diode model of the solar PV array.

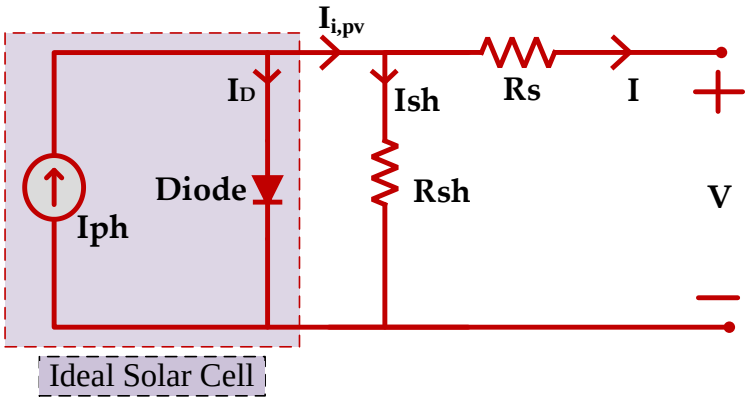

Figure 4. Single diode model of the solar PV array.

Figure 5 depicts a series-connected solar photovoltaic system with two modules.

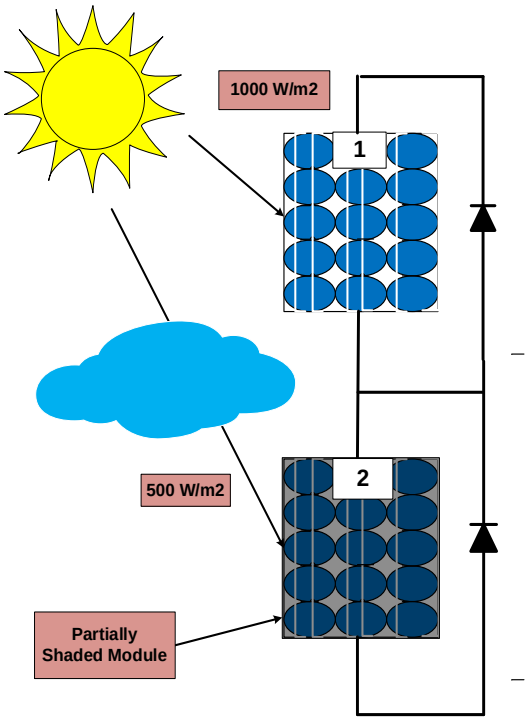

Figure 5. Solar PV array under partially-shaded-for-two Module.

The impact of partial shading on a PV array can be mathematically described using various models and equations. One of the fundamental models used to understand the

behavior of shaded PV modules is the "single diode model," which accounts for the physical processes that occur within a PV cell.

Let us consider a simplified scenario of a PV array consisting of two solar panels (Panel A and Panel B) in a series that is shown in Figure 5, with each described using the single diode model. The total current produced by the array (I_{total}) is the sum of the currents generated by each panel:

$$I_{total} = I_A + I_B \quad (1)$$

where:

I_A is the current generated by Panel A;
I_B is the current generated by Panel B.

The current generated by each panel can be further expressed using the single diode model equation:

$$I_A = I_{ph} - I_d\left(e^{q(\frac{V+IR_s}{nN_sV_T})} - 1\right) - \frac{V + IR_s}{R_{sh}} \quad (2)$$

$$I_B = I_{ph} - I_d\left(e^{q(\frac{V+IR_s}{nN_sV_T})} - 1\right) - \frac{V + IR_s}{R_{sh}} \quad (3)$$

where:

I_{ph} is the photo-generated current;
I_d is the diode current;
q is the elementary charge (1.6×10^{-19} C);
V is the voltage across the cell;
n is the ideality factor;
N_s is the number of cells in a series;
V_T is the thermal voltage ($k \times T$ / q, where k is Boltzmann's constant, and T is the temperature in Kelvin);
R_s is the series resistance;
R_{sh} is the parallel resistance or shunt resistance.

When partial shading occurs on a PV array, the behavior of shaded panels deviates from unshaded panels due to non-uniform current and voltage distributions. The shaded panels generate less current, which can lead to reverse bias conditions, causing power loss and potential hotspots.

In Figure 5, the insolation that Module 1 obtains from the sun is complete, i.e., full insolation of since 1000 W/m^2, as there are no obstructions in its path, such as clouds or buildings. In Module 2, the insolation capped at 500 W/m^2 since the cloud acts as a barrier to the sun's rays. As a result of this impact of partial shade, the solar PV module in question developed hotspots, which leads to the occurrence of localized heating. This localized heating is the cause of the damage that was done to the solar PV cell, and it also resulted in significant power losses. The output terminals of the solar module had bypass diodes attached to them so that power losses could be eliminated. These diodes have the ability to bypass the current of the afflicted module; however, doing so results in a reduction in the maximum power available at the output. Additionally, multiple power peaks develop when looking at the output. The issue is very non-linear since it has several peaks of power as it is being produced. In the literature, a number of different algorithms have been employed in order to address issues of this non-linear nature. Conventional algorithms are able to effectively follow MPP in non-shading conditions, but they are unable to track the maximum power in partially shaded conditions and become stuck at local MPP. Therefore, in this paper, an atomic orbital search algorithm was proposed that effectively tracked the MPP without getting struck by local MPP, and the purpose of this was to obtain the MPP.

3. Atomic Orbital Search (AOS) Algorithm

AOS is a computational method used in quantum chemistry for the calculation of the electronic structure of atoms and molecules. The AOS algorithm is based on the solution of the Schrödinger equation, which describes the behavior of electrons in a system. The Schrödinger equation is a partial differential equation, which cannot be solved exactly for most systems of interest. Therefore, approximate methods are used to solve the equation, and the AOS algorithm is one such method. The AOS algorithm starts by assuming that the electronic wave function of the system can be represented by a linear combination of atomic orbitals (LCAO), which are the solutions of the Schrödinger equation for isolated atoms. These atomic orbitals are also referred to as basic functions. The coefficients of the LCAO are then determined by solving the secular equation, which is a matrix equation. The secular equation is derived from the Schrödinger equation by inserting the LCAO ansatz into the equation and applying the variational principle. The variational principle states that the energy of the system is minimized when the wave function is chosen to be a member of a set of functions called the trial functions [38].

The AOS algorithm can be divided into two steps: the initialization step and the self-consistency step. In the initialization step, the atomic orbitals are chosen, and the secular equation is solved for the first time. In the self-consistency step, the secular equation is solved iteratively until the coefficients of the LCAO converge to a certain threshold. The choice of atomic orbitals is important in the AOS algorithm, as it can affect the accuracy and efficiency of the calculation [38]. The most common choice of atomic orbitals is Gaussian type orbitals (GTO), which are functions that are defined by a Gaussian function multiplied by a polynomial. GTOs are chosen due to their mathematical simplicity and flexibility. They are also easy to integrate and can be used to represent both valence and core orbitals. Another common choice is Slater type orbitals (STO), which are defined by a radial function multiplied by a polynomial. STOs are more physically motivated than GTOs, but they are less flexible [39].

The AOS algorithm is a powerful tool for the calculation of the electronic structure of atoms and molecules. It has been used to study a wide range of systems, including small molecules, large biomolecules, and solids. The method is relatively easy to implement and is well suited for parallel computing. However, the AOS algorithm has some limitations. One of the main limitations is that it is based on the LCAO approximation, which may not be accurate for systems with a large electron correlation. Another limitation is that the AOS algorithm is computationally intensive, which can make the calculation time-consuming for large systems [40]. In conclusion, the atomic orbital search algorithm is a powerful computational method used for the calculation of the electronic structure of atoms and molecules. The method is based on the solution of the Schrödinger equation and the LCAO approximation, and it involves the choice of atomic orbitals, the solution of the secular equation, and the self-consistency step.

The comparison of the quantum staircase draws a parallel to the electron's progression across distinct orbitals, achieved through energy level alterations. In cases where an electron assimilates energy beneath its binding threshold, it advances to a higher energy level in the outer orbital. Conversely, if an electron absorbs energy surpassing its binding limit, it shifts to a lower energy tier within the inner orbital. This representation of electrons' orbital movement around the atomic nucleus is illustrated in Figure 6 using the quantum staircase analogy.

AOS is an algorithm based on a population. Thus, the number of possible solutions (Y) is represented by the number of electrons in the nucleus's orbitals, and the search space is imagined as the volume of electrons around the nucleus, partitioned into thin, spherical, and concentric layers. Other choice variables $\left(y_i^j\right)$ are typically used to characterize the position of solution candidates in the search space, whereas the solution candidate $\left(Y_i^k\right)$ expresses the ith electron in the kth imaginary layer.

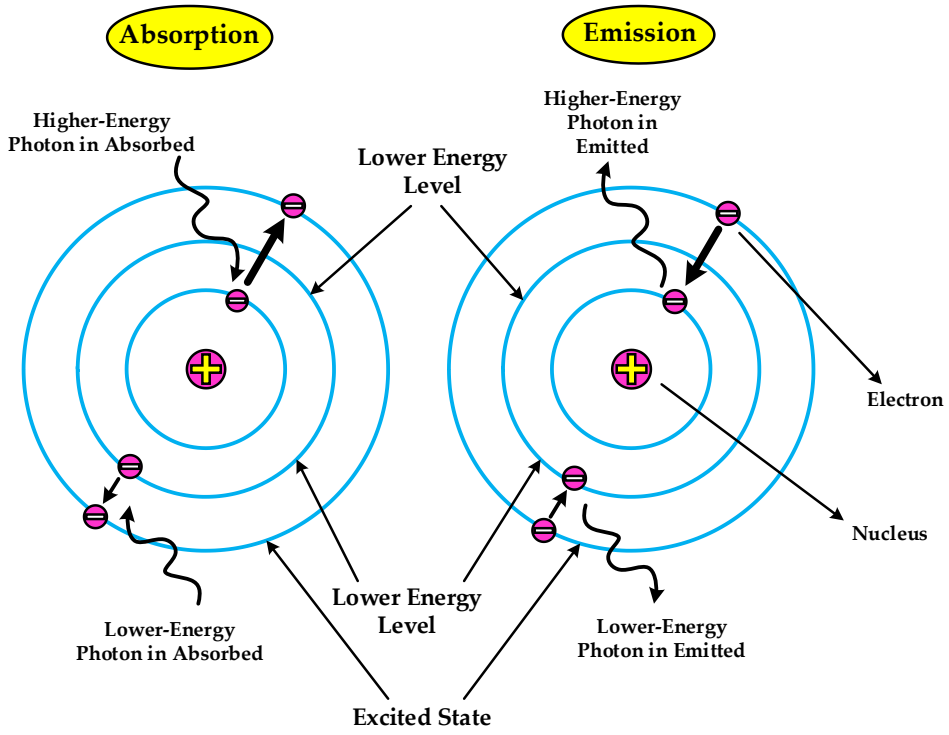

Figure 6. The quantum staircase comparison pertaining to electrons encircling the atomic nucleus.

The hypothetical spherical layers (L) in the vicinity of the nucleus, which also display the quantum number, are represented by the integer value n in order to mathematically explain the atomic orbital model. The nucleus layer L_o of the smallest radius R_o represents the absence of electrons and the presence of just the nucleus in this layer. The electron probability diagram is taken into account by the probability density function (PDF), which uses it to determine the location of the electron (solution candidate) around the nucleus.In this case, mathematical modeling uses the energy state of an electron as an objective value function. Better objective-value solution candidates (electrons) stand out at lower energy levels (LE^k), but inferior objective-value functions are taken into account at higher energy levels. The diagram in Figure 7a,b illustrates the process of locating potential solution candidates (electrons) within imaginary layers using a PDF based on a standard Gaussian distribution. It is important to highlight that the overall likelihood of locating an electron in the second imaginary layer is greater than that in the first layer. Consequently, the PDF for the second layer (spanning from L_1 to L_2) exhibits higher values compared to the first layer (spanning from L_0 to L_1).

Greater *PDF* values are seen as a superior objective value function, indicating that the electrons are positioned in the inner electron layers and have lower energy levels (LE^k). The lower *PDF* values similarly imply a poorer objective value function, meaning that electrons are located in hypothetical outer layers with greater energy levels. As depicted in Figure 7, the nucleus layer is employed to place the leading entity (LE), which possesses the most favorable objective function value among all potential solution candidates.

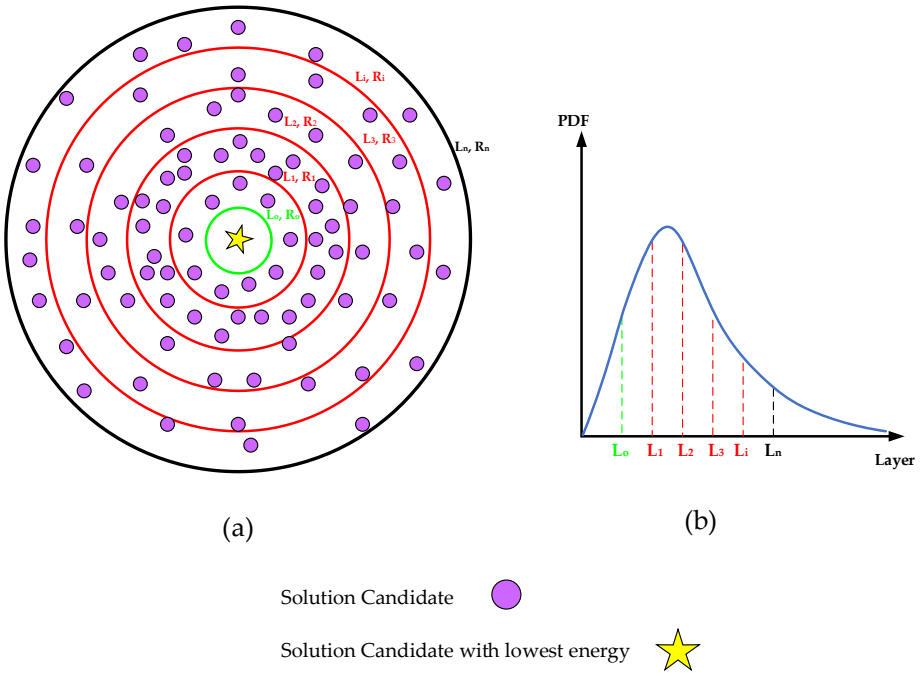

Figure 7. Defining the position of solution candidates via PDF in a graphical format.

E^k is the symbol for the value of the objective function that matches the solution candidate, which is an electron, in the kth hypothetical layer. The following math equation [38] is used to randomly choose where the electrons, also called solution candidates, start in the search space:

$$y_1^j(0) = y_{i,min}^j + rand.\left(y_{i,max}^j - y_{i,min}^j\right), \quad \begin{cases} i = 1,\ 2, \ldots, m \\ j = 1,\ 2, \ldots, d \end{cases} \tag{4}$$

As a result, the following mathematical equations are created:

$$Y^k = \begin{bmatrix} Y_1^k \\ Y_2^k \\ \vdots \\ Y_i^k \\ \vdots \\ Y_p^n \end{bmatrix} = \begin{bmatrix} y_1^1 & y_1^2 & \ldots & y_1^i & \ldots & y_1^d \\ y_2^1 & y_2^2 & \ldots & y_2^i & \ldots & y_2^d \\ \vdots & & & \vdots & & \vdots \\ y_i^1 & y_i^2 & \ldots & y_i^i & \ldots & y_i^d \\ \vdots & & & \vdots & & \vdots \\ y_p^1 & y_p^2 & \ldots & y_p^i & \ldots & y_p^d \end{bmatrix}, \quad \begin{cases} i = 1, 2, \ldots, p \\ j = 1, 2, \ldots, d \\ k = 1, 2, \ldots, n \end{cases} \tag{5}$$

$$E^k = \begin{bmatrix} E_1^k \\ E_2^k \\ \vdots \\ E_i^k \\ \vdots \\ E_p^n \end{bmatrix}, \quad \begin{cases} i = 1,\ 2, \ldots, p. \\ k = 1,\ 2, \ldots, n. \end{cases} \tag{6}$$

E_i^k is the notation used to indicate the value of the objective function that corresponds to the ith solution candidate (electron) in the kth hypothetical layer. The entire number of candidate solutions (electron) in the kth hypothetical layer is represented by the symbol 'p', while the dimension of the problem is represented by the symbol 'd'. The binding energy (BE) and binding state (BS) of the hypothetical kth layer are formulated as the mean

of all candidate solution (electrons') locations and objective function values in a specific layer [41], as described in the following manner:

$$BS^k = \frac{\sum_{i=1}^{p} Y_i^k}{p}, \quad \begin{cases} i = 1, 2, \ldots, p. \\ k = 1, 2, \ldots, n. \end{cases} \tag{7}$$

$$BE^k = \frac{\sum_{i=1}^{p} E_i}{p}, \quad \begin{cases} i = 1, 2, \ldots, p. \\ k = 1, 2, \ldots, n. \end{cases} \tag{8}$$

In a similar manner, the average coordinates and objective function values of all of the candidate solutions in the search space were utilized to formulate the following equations [41] for determining an atom's binding state and binding energy:

$$BS = \frac{\sum_{i=1}^{m} Y_i}{m}, \quad i = 1, 2, \ldots, m. \tag{9}$$

$$BE = \frac{\sum_{i=1}^{m} E_i}{m}, \quad i = 1, 2, \ldots, m. \tag{10}$$

where Y_i and E_i represent, respectively, the location of the ith solution candidate (electron) in the atom and the value of the objective function for that candidate. The symbol 'm' is used to represent the total number of candidate solutions (electrons) that may be found in the search space. In order to quantitatively depict the effect of the photon on the electrons that are located surrounding the nucleus, a random integer with a uniform distribution, denoted by the symbol 'θ', is generated in the range of (0 to 1) for each possible solution (an electron). As a parameter, the photon rate (PR) may be used to calculate the chance that a photon will interact with an electron.

If the value is greater than or equal to PR, then the movement of electrons is determined by the emission and absorption of photons. To determine whether a photon is emitted, the energy level (E_i^k) of each electron (represented as Y_i^k) is compared to the binding energy (BE^k) of the corresponding hypothetical layer. If E_i^k is greater than or equal to BE^k, a photon is emitted, and the electron moves to the state with the lowest energy level (LE) in the atom, which simultaneously reaches the binding state of the atom (BS) [41]. The electron's position is updated mathematically as:

$$Y_i^{k+1} = Y_i^k + \frac{\sigma_i \times (\omega_i \times LE - \varphi_i \times BS)}{k}, \quad \begin{cases} i = 1, 2, \ldots, p. \\ k = 1, 2, \ldots, n. \end{cases} \tag{11}$$

If the value of E_i^k is less than BE^k, it suggests that the electron and photon have both arrived at the binding state (BS^k), and the state with the lowest energy level (LE^k) of the kth layer at the same time. The position is then updated according to the following mathematical expression:

$$Y_i^{k+1} = Y_i^k + \sigma_i \times \left(\omega_i \times LE^k - \varphi_i \times BS^k\right), \quad \begin{cases} i = 1, 2, \ldots, p. \\ k = 1, \ldots\ldots, n. \end{cases} \tag{12}$$

The position of the ith solution candidate in the kth layer is updated by using Y_i^{k+1} as the next position and Y_i^k as the current position. To determine the amount of energy emitted or absorbed, randomly produced vectors σ_i, ω_i, and φ_i, which are uniformly distributed in the range of (0,1), are used.

If the value of θ is less than PR, then it is impossible to predict the effect of a photon on an electron. The electron's movement between different layers depends on its interaction

with other particles or magnetic fields. Therefore, the position of the solution candidate is updated accordingly using Equation (13):

$$Y_i^{k+1} = Y_i^k + r_i \ , \quad \begin{cases} i = 1,\ 2, \ldots, p. \\ k = 1,\ 2, \ldots, n. \end{cases} \tag{13}$$

where Y_i^k and Y_i^{k+1} are the current position and next position for the ith candidate solution of the kth layer, respectively; r_i is a randomly generated and uniformly distributed vector in the range of (0,1). The AOS algorithm's pseudocode is displayed in Algorithm 1.

Algorithm 1. seudocode of AOS algorithm.

START

- Initialization of positions of solution candidates (Y_i) in the search space with m candidates.
- Calculation of Fitness objective value (E_i) for initial solution candidates.
- Determine Binding Energy (BE) and Binding State (BS) of an atom.
- Find the candidate with Lowest Energy level (LE) in an atom.

while iter < maximum number of iterations

- Create ***n*** as number of hypothetical layers around nucleus
- Sort *solution candidates* in descending order
- Allocate *solution candidates* in the hypothetical layers by PDF

for k = 1 : n

- Determine Binding Energy (BE^k) and Binding State (BS^k) of the k^{th} layer.
- Find the candidate with Lowest Energy level (LE^k) in the k$^{\text{th}}$ layer.

for $i = 1 : p$

- Approximate $\theta,\ \sigma,\ \omega,\ \varphi$
- Estimate PR

if $\theta \geq PR$

if $E_i^k \geq BE^k$

$$Y_i^{k+1} = Y_i^k + \frac{\sigma_i \times (\omega_i \times LE - \varphi_i \times BS)}{k}$$

else if $E_i^k < BE^k$

$$Y_i^{k+1} = Y_i^k + \sigma_i \times \left(\omega_i \times LE^k - \varphi_i \times BS^k\right)$$

end

else if $\theta < PR$

$$Y_i^{k+1} = Y_i^k + r_i$$

end

end

end

- Update Binding Energy (BE) and Binding State (BS) of an atom.
- Update candidate with lowest energy level in an atom (LE)

end while

STOP

4. Maximum Power Tracking in Solar PV System

The motivation and inspiration behind utilizing the atomic orbital search (ASO) algorithm in our research stem from its unique and promising characteristics, which align well with the challenges posed by maximum power point tracking (MPPT) in partially shaded solar photovoltaic (PV) systems. ASO draws its inspiration from the principles of atomic and molecular interactions, which provide a metaphorical framework for optimizing complex problems. This algorithm leverages the concept of atomic orbitals and their interactions to guide the search for optimal solutions in a continuous search space. The ASO algorithm's ability to adapt and explore intricate landscapes aligns with the nuanced and dynamic nature of MPPT in partially shaded conditions, where the traditional algorithms often struggle to strike a balance between exploration and exploitation. ASO's capacity to

address non-linearity and multi-modal behavior, characteristics of PV power generation under varying shading conditions, makes it a compelling candidate for improving MPPT performance. The novel nature of ASO, along with its potential to overcome challenges unique to partially shaded environments, has motivated our exploration of its applicability in enhancing energy capture and overall system efficiency.

The switching of the boost converter decides the power received by the load. For tracking maximum power, the switching of the boost converter is set to some value for which the power received by the load will be maximum. The particular value of the duty ratio, which corresponds to the maximum power, is found by using various algorithmic techniques. The algorithms are developed on a software platform, such as MATLAB, and then embedded in a microprocessor. The voltage and current are given as input to the microprocessor, and in place, it provides a duty ratio to the boost converter switch in pulsated form. The pulse corresponding to the duty ratio is obtained using a gate driver circuit. The algorithms are designed such that in every iteration the duty ratio is updated by using the equations involved in the algorithm. The previously stored power is then compared with the power that is newly obtained at the load corresponding to the new duty ratio. If the previously stored power proves to be higher than the newly tracked power, then the new duty ratio is discarded, and the previously stored duty ratio is preserved.

Finally, after numerous iterations, the duty ratio becomes constant. That constant duty ratio is the duty ratio corresponding to the maximum power. Hence, in this way, the maximum power of the solar PV array is tracked.

The fitness function for the proposed AOS algorithm is as follows:

$$I_T = I_{ph} - I_d\left(e^{\frac{V+IR_S}{nV_T}} - 1\right) - \frac{V + IR_s}{R_{sh}} \tag{14}$$

$$P = I_T \times V \tag{15}$$

where I_T represents the total current in the circuit, I_{ph} denotes the photocurrent generated by the photovoltaic (PV) cell, I_d stands for the saturation current of the diode, V represents the voltage across the PV cell, I denotes the total current in the circuit, R_s represents the series resistance, n denotes the ideality factor of the diode, V_T represents the thermal voltage of the diode, R_{sh} stands for the shunt resistance, and P represents the power output of the PV cell.

For a detailed explanation of MPPT utilizing AOS, the below steps represent the basic implementation of the AOS algorithm for MPPT tracking in solar PV systems.

STEP 1-Initialization

In this step, the initial population of atomic orbitals is generated randomly. Each atomic orbital represents a possible solution to the MPPT problem.

STEP 2-Fitness evaluation

In this step, the fitness value of each atomic orbital in the population is evaluated. The fitness value is a measure of how well the atomic orbital fits the experimental data. The fitness value is calculated using an objective function that measures the deviation between the measured power and the power predicted by the atomic orbital.

STEP 3-Selection

In this step, the best atomic orbitals in the population are selected based on their fitness value. The selection process is based on the principle of survival of the fittest.

STEP 4-Mutation

In this step, the selected atomic orbitals are mutated by applying a perturbation to their values. The perturbation is used to explore the search space and find new solutions that are not present in the initial population.

STEP 5-Termination

In this step, the algorithm stops when a termination criterion is met. The termination criterion of the algorithm is the maximum number of iterations (Tmax), where Tmax is equal to 100 and also ($T \leq$ Tmax).

STEP 6-Update

In this step, the best solution found by the algorithm is updated as the current solution. The algorithm then returns to step 2 to continue the search for the optimal solution.

The flowchart for the AOS algorithm is illustrated in Figure 8.

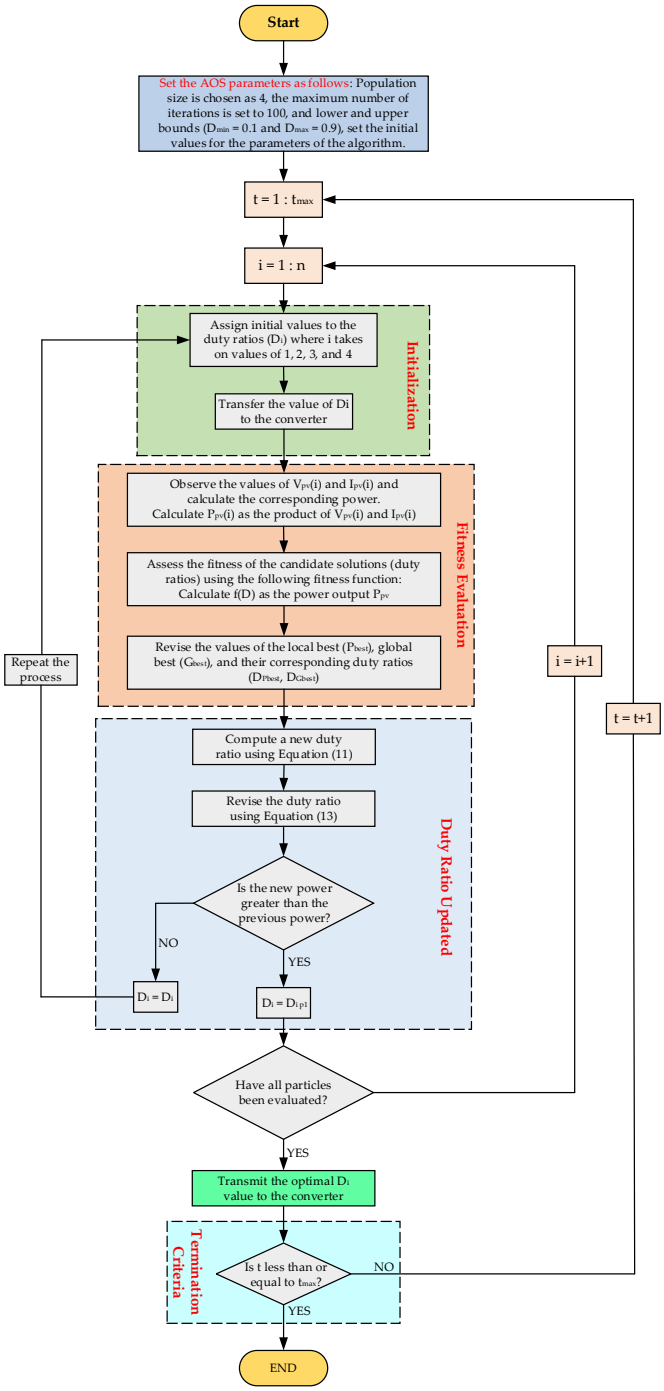

Figure 8. Flowchart depicting MPPT in a solar PV system using optimization based on the atomic orbital search algorithm.

5. Results and Discussion

The complete setup for circuit realization in real-time using Typhoon HIL (402) for the algorithms is shown in Figure 9. The setup consisted of a solar PV array, which was made up of four modules connected in series, which were used for providing input voltage and current to the DC-DC boost converter; a DC-DC boost converter was used as a medium between PV array and output load; and a voltage sensor and current sensor were used for measuring the voltage and current of the panel. The measured quantity was sent to the controller, which sent pulse width modulation (PWM) signals to the gate driver.

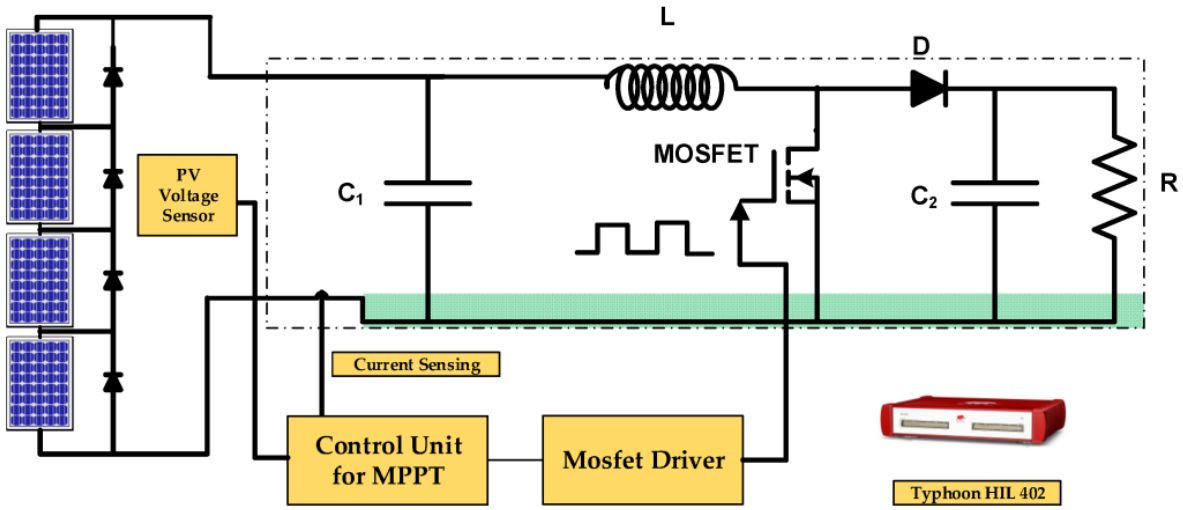

Figure 9. Circuit Realization for MPPT in Typhoon HIL.

The ratings of various components of boost converter were as follows: inductance (L) = 1.1478 mH, input capacitance (C_i) = 47 µF , output capacitance (C_o) = 470 µF, and output load (R) = 10 Ω. The specifications of the components used are also represented in tabular form, as shown in Table 2. A solar PV array with a standard rating is shown in Table 3. The various parameters of a module of the array are as follows: maximum power (P_{MPP}) = 21.837 watts, open circuit voltage (V_{OC}) = 5.425 volts, short circuit current (I_{SC}) = 5.34 ampere, voltage at maximum power (V_{MPP}) = 4.35 volts, and current at maximum power (I_{MPP}) = 5.02 ampere. The array chosen consisted of four modules, and hence, the maximum power rating of the array became 87.348 watts. The gate driver received the updated duty ratio after each iteration in the form of modulated pulses, which activated the switch and transferred the associated optimised power—the sum of the optimised voltage and current—to the output load. The suggested technique is compared to other state-of-the-art algorithms for various PS circumstances in the next section.

Table 2. Specification of the circuit parameter.

Parameter	Unit	Values
Inductance (L)	mH	1.1478
Input capacitance (C_i)	µF	47
Output capacitance (C_o)	µF	470
Output load (R)	Ω	10

Table 3. Specifications of the PV array.

Parameter	Unit	Value
PV module in series	-	4
PV module in parallel	-	1
PV cells per module	-	72
Open-circuit voltage (V_{oc})	Volts	5.425
Short-circuit current (I_{sc})	Amperes	5.34
Voltage at maximum power point (V_{mpp})	Volts	4.35
Current at maximum power point (I_{mpp})	Amperes	5.02
Maximum power (P_{mpp})	Watts	21.837
Temperature coefficient of V_{oc} (K_v)	%/°C	−0.37501
Temperature coefficient of I_{sc} (K_i)	%/°C	0.075

Table 4 compiles the insolation conditions employed in the simulation studies. The provided table presents information concerning insolation conditions, measured in watts per square meter (W/m^2), for four distinct scenarios labeled as G_1, G_2, G_3, and G_4, alongside the associated rated power, which signifies the maximum power output in watts (W) of the PV modules. When subjected to the ideal condition of standard insolation amounting to 1000 W/m^2, all four modules attained their rated power of 87.26 W (G_1: 1000 W/m^2, G_2: 1000 W/m^2, G_3: 1000 W/m^2, and G_4: 1000 W/m^2). However, as insolation levels declined, the rated power diminished proportionally. For instance, in condition 1, the panels received less insolation (G_1: 1000 W/m^2, G_2: 800 W/m^2, G_3: 600 W/m^2, and G_4: 400 W/m^2), resulting in a rated power of 40.99 W. The data underscore the clear correlation between insolation and the performance of PV modules, underscoring the significance of comprehending and accounting for insolation levels when evaluating the energy output of a photovoltaic system across diverse conditions. The shading patterns applied to the modules can have a significant impact on the performance of the solar PV system. When a solar PV module is shaded, the shaded cells generate less power, which can reduce the overall power output of the system.

Table 4. Various shading patterns on four modules.

	Values of Insolation (W/m^2)				
Condition	**Panel 1 (G_1)**	**Panel 2 (G_2)**	**Panel 3 (G_3)**	**Panel 4 (G_4)**	**Rated Power (W)**
1	1000	800	600	400	41.02 W
2	1000	900	650	500	50.50 W
3	1000	1000	800	400	45.20 W
4	1000	1000	1000	1000	87.26 W

Table 5 presents the control parameters for the optimization techniques employed in this study. The chosen techniques include AOS, Cuckoo Search, JAYA, and Phasor-PSO. For each technique, specific control parameters were used to guide the optimization process. These parameters included population size (N), maximum number of iterations (T_{max}), and additional parameters unique to each technique. In the case of atomic orbital search, the parameters also encompassed orbital radius (r) and decay rate (α). For Cuckoo Search, the parameters involved Parameter β and probability of discovery (p_a). JAYA employed exploration rate (C_r) and learning rate (C_s) as its control parameters. Phasor-PSO utilized inertia weight (w), cognitive factor (c_1), and social factor (c_2) for its optimization process. The specified values used for each parameter in this study are outlined in Table 5, aiding in replicating and comprehending the experimental setups for further analysis and interpretation.

Table 5. The control parameters of the optimization techniques employed in this study.

Optimization Techniques	Control Parameters	Values Used
Atomic Orbital Search	Population size (N), maximum number of iterations (T_{max}), orbital radius (r), decay Rate (α).	$N = 4$, $T_{max} = 100$, $r = 0.5$, $\alpha = 0.999$
Cuckoo Search	Population size (N), maximum number of iterations (T_{max}), Parameter β, probability of discovery (p_a).	$N = 4$, $T_{max} = 100$, $\beta = 1.5$, $p_a = 0.3$
JAYA	Population size (N), maximum number of iterations (T_{max}), exploration rate (C_r), learning rate (C_s).	$N = 4$, $T_{max} = 100$, $C_r = 0.1$, $C_s = 0.9$
Phasor-PSO	Population size (N), maximum number of iterations (T_{max}), inertia weight (w), cognitive factor (c_1), social factor (c_2).	$N = 4$, $T_{max} = 100$, $w = 0.7$, $c_1 = 1.5$, $c_2 = 2.0$

The simulation experiments involved a comprehensive investigation of diverse insolation values, as visually depicted in Figure 10a–d. This exploration resulted in the emergence of distinct shapes and peaks observed in the photovoltaic (P-V) characteristics. Figure 10 also provides valuable insights into the presence and significance of the bypass diode (D_{bp}) and the blocking diode (D_{bk}) within the photovoltaic system. Through this simulation, the distinctive roles of these diodes are highlighted, with the bypass diode facilitating the redirection of current flow during varying insolation conditions and the blocking diode preventing undesired reverse current flow.

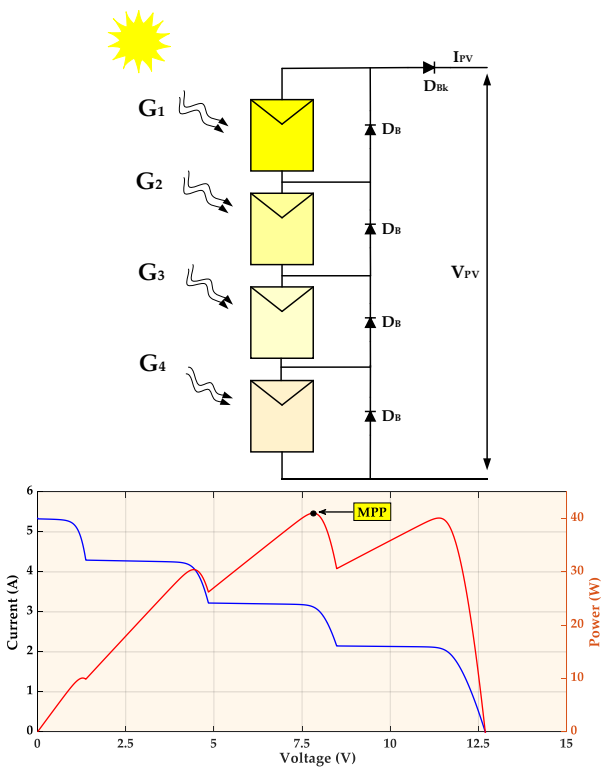

Condition 1
MPP = 41.02 W
(**a**)

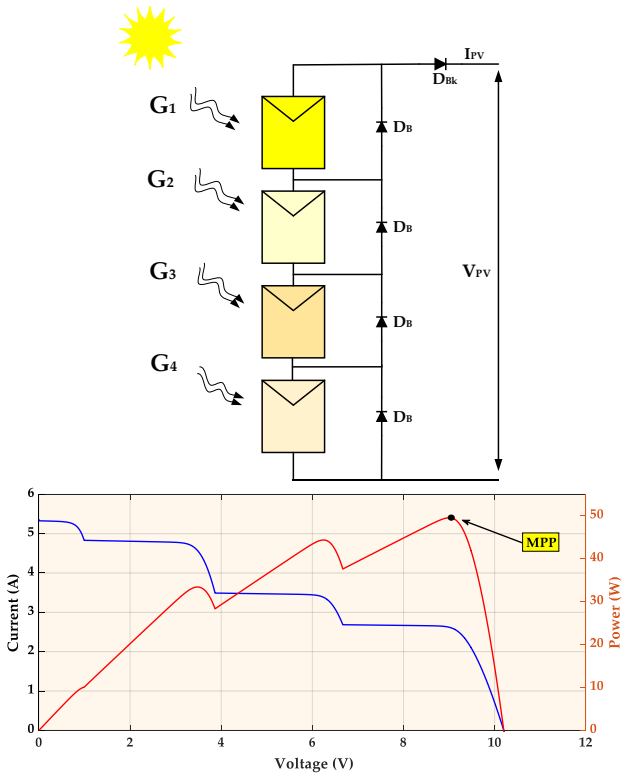

Condition 2
MPP = 50.50 W
(**b**)

Figure 10. *Cont.*

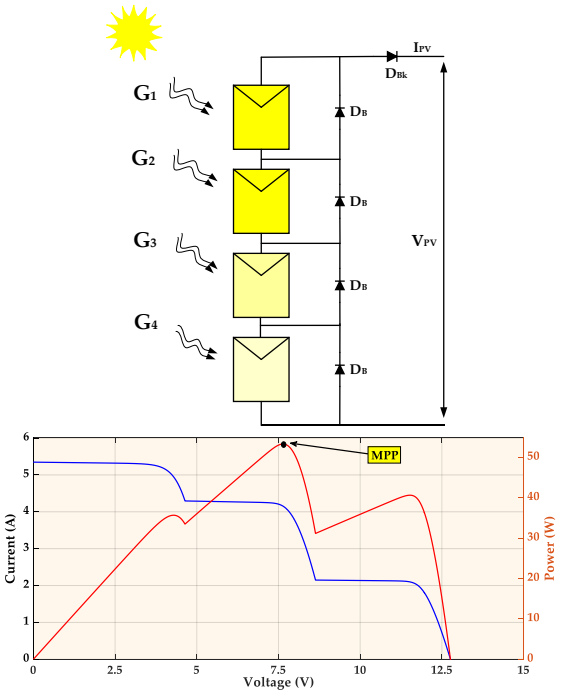

Condition 3
MPP = 45.20 W
(**c**)

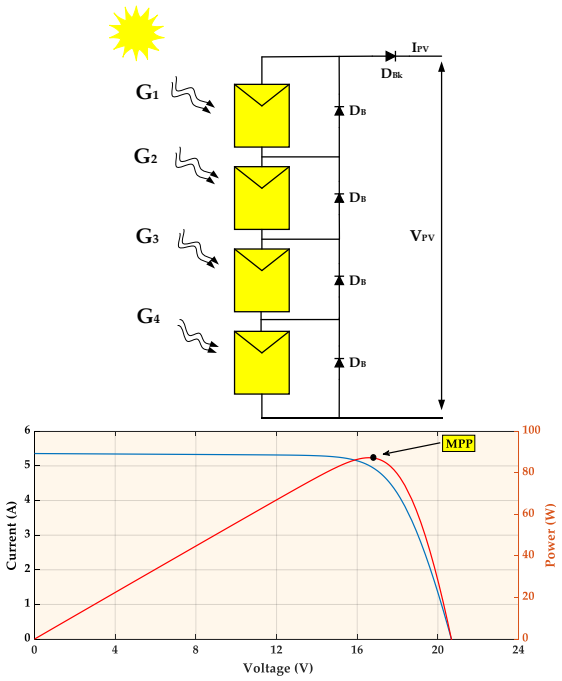

Condition 4
MPP = 87.26 W
(**d**)

Figure 10. (**a**–**c**) Four PV modules received different values of solar irradiance; (**d**) four PV modules received equal irradiance, i.e., full solar irradiance.

Table 6 presents a concise comparison of four algorithms, offering insights into their performance based on both convergence time and efficiency under different solar irradiance conditions. To better understand the implications of these results, the significance of the findings is described below.

Table 6. Summary of the comparison of four algorithms based on convergence time and efficiency.

Algorithms	Condition 1 (1000 800 600 400) W/m^2		Condition 2 (1000 900 650 500) W/m^2		Condition 3 (1000 1000 800 400) W/m^2		Condition 4 (1000 1000 1000 1000) W/m^2	
	Convergence Time (Sec)	Efficiency (%)	Convergence Time (Sec)	Efficiency (%)	Convergence Time (Sec)	Efficiency (%)	Convergence Time (Sec)	Efficiency (%)
JAYA	2.10	96.48	2.20	96	2.20	97.77	7.2	97.26
Phasor-PSO	1.90	96.70	4.00	98.10	3.40	93.68	0.80	97.83
Cuckoo Search	4.80	97.50	4.00	99.24	2.80	94.40	8.00	97.41
AOS [proposed]	1.80	97.58	1.00	99	1.90	96.52	1.10	98.55

The 'convergence time' column serves as a measure of the time taken by each algorithm to achieve convergence or to identify the maximum power point. It also refers to the duration taken by a metaheuristic optimization algorithm to converge to an optimal or near-optimal solution for a given problem. It represents the computational effort required by the algorithm to explore the solution space, locate a solution that meets the optimization criteria, and measure the speed at which the algorithm finds an acceptable solution. Efficiency in the context of metaheuristic optimization algorithms pertains to the quality of the solutions generated relative to the computational resources expended. It signifies how well an

algorithm can approach the optimal solution, given the available time and computational power. A highly efficient algorithm produces solutions that are close to the global optimum while utilizing a reasonable amount of computational effort.

Condition 1 (1000 800 600 400) W/m^2: In the context of the initial solar irradiance scenario, the provided table reveals fascinating insights into the performance of the four optimization algorithms. Among them, "AOS" stood out with a convergence time of 1.80 s and an impressive efficiency of 97.58%. These results signify that the "AOS" algorithm adeptly balanced the need for swift convergence with the extraction of optimal power from solar panels. "Phasor-PSO" followed closely, exhibiting a convergence time of 1.90 s and an efficiency of 96.70%. Although it took slightly more time to converge compared to "AOS," "Phasor-PSO" maintained an efficiency that showcases its ability to effectively extract power even in this variable irradiance condition. "Jaya" presented a convergence time of 2.10 s and an efficiency of 96.48%, indicating its relatively stable performance across both convergence time and power extraction. Meanwhile, "Cuckoo Search" took more time to converge at 4.80 s but maintained a high efficiency of 97.50%, revealing a trade-off between convergence speed and power extraction efficiency.

Condition 2 (1000 900 650 500) W/m^2: Transitioning to a scenario with higher solar irradiance, "Phasor-PSO" continued to demonstrate remarkable efficiency with a convergence time of 4.00 s and the highest efficiency of 98.10%. This outcome underscored "Phasor-PSO's" prowess in optimizing power extraction, even in conditions with greater solar intensity. Notably, "Cuckoo Search" maintained its convergence time of 4.00 s while achieving an impressive efficiency of 99.24%. This remarkable efficiency speaks to its ability to achieve solutions that are near-optimal under varying irradiance levels. "AOS" adapted well to the increased irradiance, displaying a significant reduction in convergence time to 1.00 s while maintaining a high efficiency of 99%. This result positioned "AOS" as a suitable choice for scenarios with heightened solar radiation, where quick convergence and effective power extraction are crucial. "Jaya" maintained its convergence time of 2.20 s, while its efficiency remained at 96.00%, reflecting its consistent performance even in changing conditions.

Condition 3 (1000 1000 800 400) W/m2: As the solar irradiance conditions shifted once again, "Jaya" and "AOS" exhibited convergence times of 2.20 s and 1.90 s, respectively. Their efficiencies remained relatively high at 97.77% and 96.52%, signifying their robustness in handling varying solar intensities. "Cuckoo Search" faced a slight decrease in efficiency to 94.40% alongside a convergence time of 2.80 s, indicating its sensitivity to the specific conditions of this scenario. Similarly, "Phasor-PSO" experienced a drop in efficiency to 93.68%, while maintaining a convergence time of 3.40 s. This suggests that the efficiency of "Phasor-PSO" is influenced by the particular attributes of this irradiance condition.

Condition 4 (1000 1000 1000 1000) W/m^2: Under the conditions of uniform high solar radiation, "Phasor-PSO" remained a strong performer, achieving a convergence time of 0.80 s and an efficiency of 97.83%. This outcome underscores its effectiveness in optimizing power extraction when solar intensity is consistently high. "AOS" maintained its efficiency at 98.55% while achieving a convergence time of 1.10 s, showcasing its ability to maintain high power extraction efficiency even in scenarios with intense irradiance. "Jaya" experienced a notable increase in convergence time to 7.20 s, potentially indicating challenges in achieving rapid convergence under such high radiation conditions. Lastly, "Cuckoo Search" exhibited a convergence time of 8.00 s and an efficiency of 97.41%, suggesting that it faced difficulties in achieving quick convergence under these conditions.

In conclusion, the proposed "AOS" algorithm consistently excelled with swift convergence times and remarkable efficiency across all states. While other algorithms may excel in certain efficiency aspects, the "AOS" algorithm balanced performance in terms of both speed and efficiency positions it as the superior choice. Moreover, no significant oscillation in size can be observed in the results of the proposed algorithm (AOS) for all four conditions (1, 2, 3, and 4) in Figure 11a–d. First, significant fluctuation is caused by duty ratio initialization and has no impact on the effectiveness of the algorithm; thus, it

is not regarded as a fluctuation. Another advantage of small, intelligent diversification is that, if the MPP is followed, the ultimate convergence choice may be made more quickly, preventing further power losses. These outcomes underscore that the "AOS" algorithm provided a compelling blend of rapid convergence and effective power extraction, establishing it as an exceptional option for maximum power point tracking across diverse scenarios. All of these factors help to significantly use the power generated by the PV array, boosting overall efficiency.

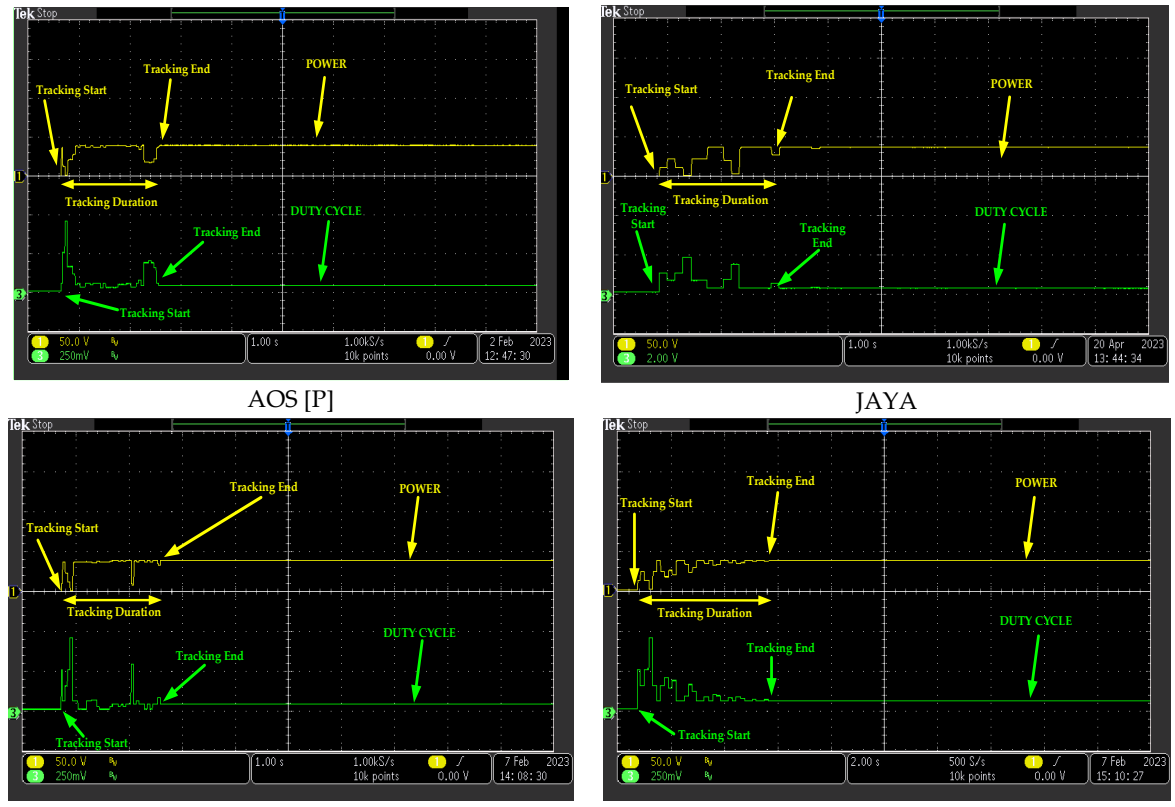

(**a**)

Figure 11. *Cont.*

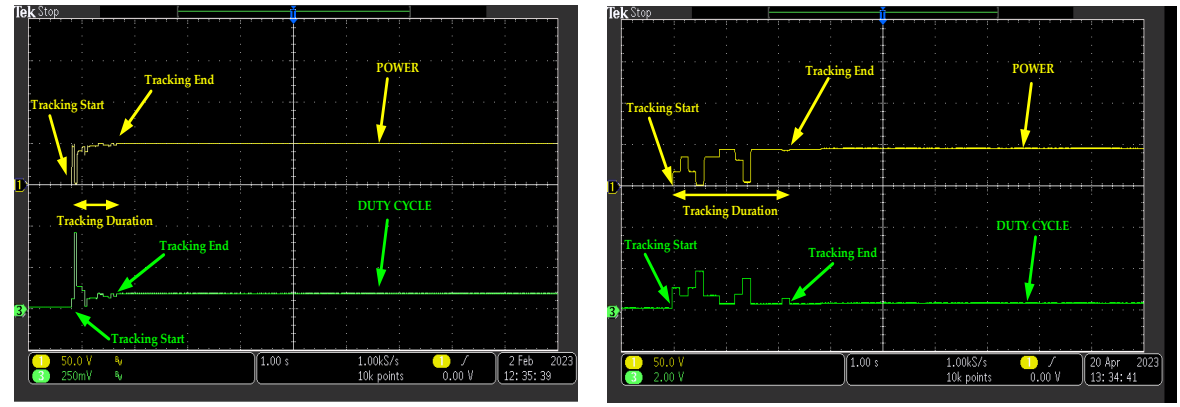

AOS [P] JAYA

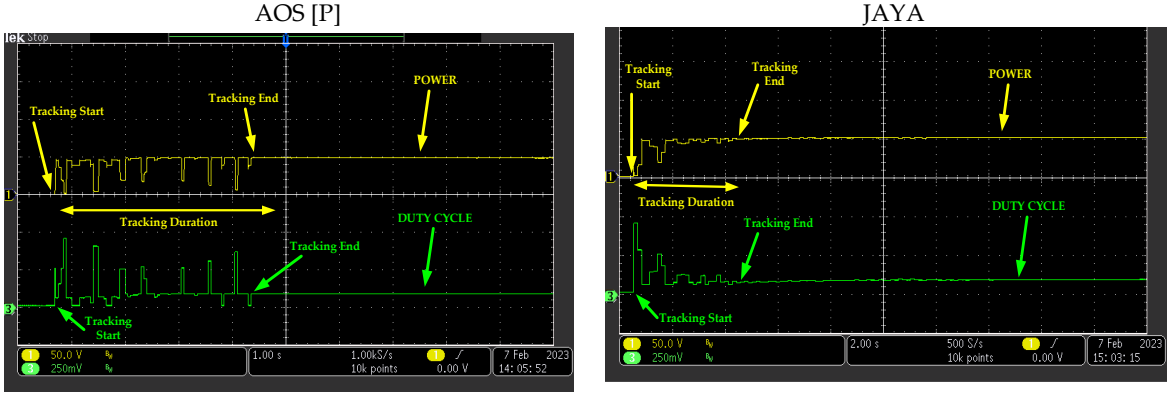

Phasor PSO Cuckoo Search

(**b**)

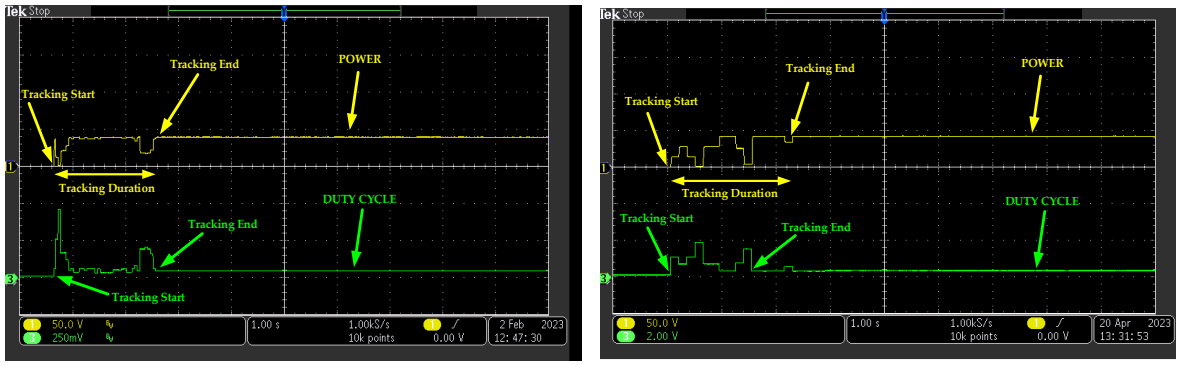

AOS [P] JAYA

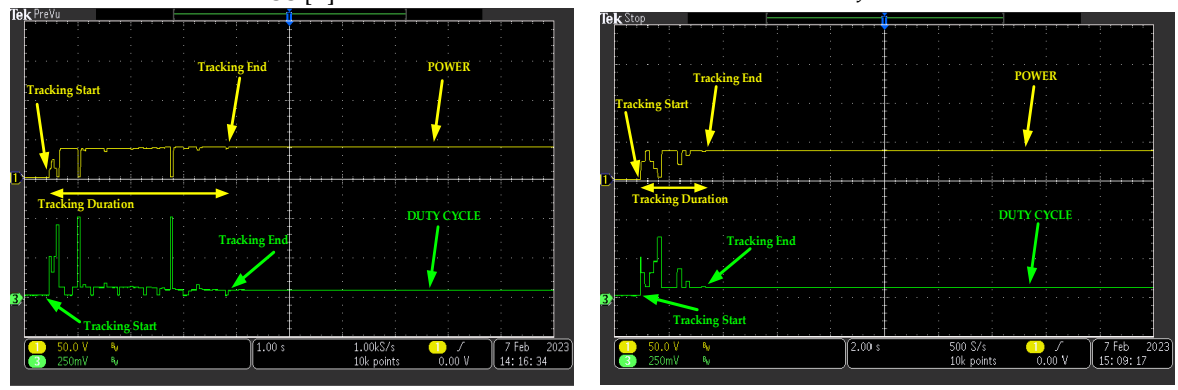

Phasor PSO Cuckoo Search

(**c**)

Figure 11. *Cont.*

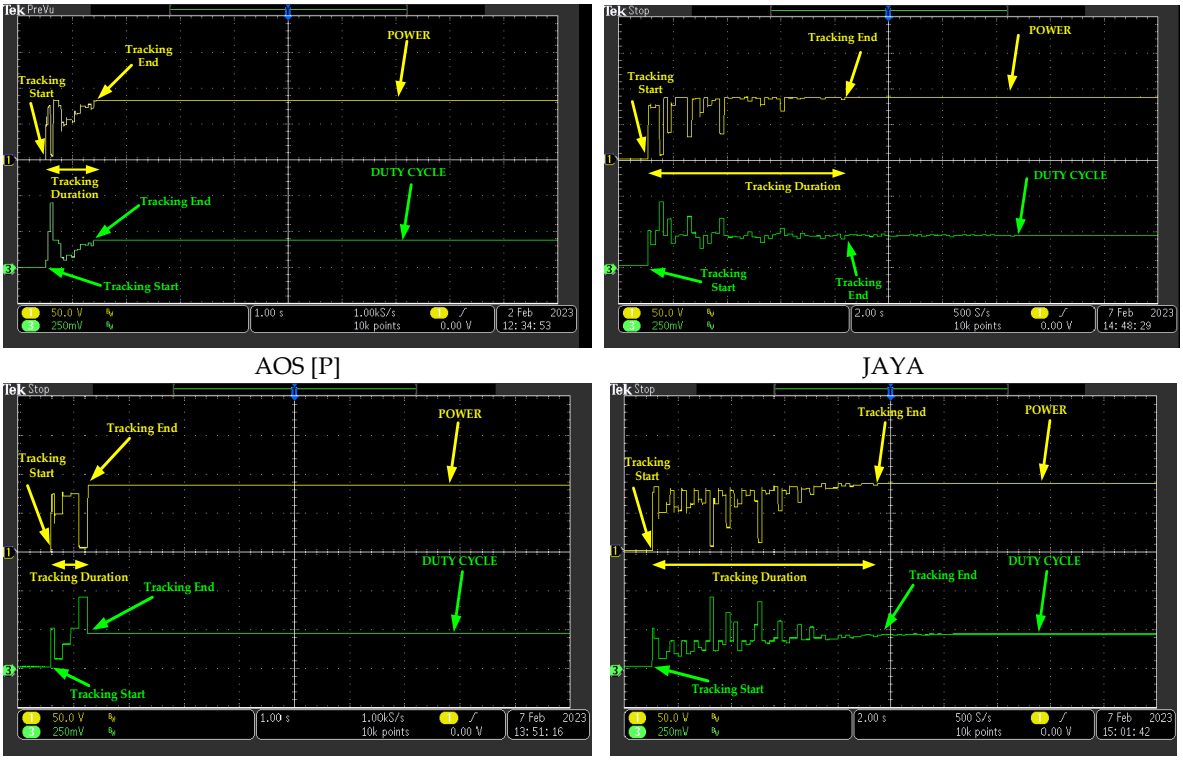

(**d**)

Figure 11. (**a**) MPPT performance comparison of the proposed algorithm with different algorithms (JAYA, Phasor-PSO, and Cuckoo Search) for condition 1 (1000, 800, 600, 400) W/m^2. (**b**) MPPT performance comparison of the proposed algorithm with different algorithms (JAYA, Phasor-PSO, and Cuckoo Search) for condition 2 (1000, 900, 650, 500) W/m^2. (**c**) MPPT performance comparison of the proposed algorithm with different algorithms (JAYA, Phasor-PSO, and Cuckoo Search) for condition 3 (1000, 1000, 800, 400) W/m2. (**d**) MPPT performance comparison of the proposed algorithm with different algorithms (JAYA, Phasor-PSO, and Cuckoo Search) for condition 4 (1000, 1000, 1000, 1000) W/m^2.

6. Conclusions

In this study, our primary objective was to devise an advanced maximum power point tracking (MPPT) controller that addresses the challenges of fluctuating power output in photovoltaic (PV) systems. Our aim was to minimize output fluctuations while enhancing tracking speed, efficiency, and overall reliability. Through rigorous experimentation and analysis, we arrived at substantial contributions that pave the way for more efficient solar energy extraction. The proposed MPPT algorithm demonstrated remarkable benefits, contributing to improved PV system performance. The algorithm's key advantages include higher efficiency, reduced tracking time, diminished output variations, and enhanced duty ratios. These combined attributes facilitate a swift convergence to the maximum power point (MPP) following monitoring, ensuring optimized energy conversion even in challenging operational scenarios. Under varying degrees of partial shading, our method underwent rigorous evaluation, benchmarked against three prominent metaheuristic algorithms, JAYA, Phasor-PSO, and the Cuckoo Search algorithm. Notably, our algorithm consistently outperformed the Phaser-PSO, JAYA, and Cuckoo Search algorithms in terms of convergence time. Furthermore, its resilience in accurately tracking the MPP, even within complex scenarios featuring narrow global-to-local optima gaps, sets it apart as a robust and efficient choice. The multifaceted benefits of our proposed approach establish it as an optimal solution for constructing highly effective MPP trackers, adaptable across industrial, commercial, and residential settings. Its capacity to enhance energy efficiency and rapidly

respond to changing conditions highlights its potential for substantial positive impact in diverse real-world applications. It is important to acknowledge that, while our work presents a significant stride forward, the domain of MPPT continues to evolve. As various algorithms compete in terms of performance and capabilities, the pursuit of superior solutions remains an ongoing endeavor. This study underscores the open and dynamic nature of MPPT research, inviting the development of innovative algorithms capable of further enhancing controller performance and contributing to the continuous optimization of renewable energy extraction.

Author Contributions: Conceptualization, M.T. and A.S.; formal analysis, M.T.H., M.T., A.S., S.U., A.B. and M.A.H.; funding acquisition, S.U. and A.B.; investigation, M.T.H., M.T., A.S. and M.A.H.; methodology, M.T.H., M.T. and A.S.; project administration, S.U. and A.B.; supervision, M.T. and A.S.; validation, M.T.H. and A.S.; writing—original draft, M.T.H., M.T. and A.S.; writing—review and editing, S.U., A.B. and M.A.H. All authors have read and agreed to the published version of the manuscript.

Funding: This research project was funded by the Deanship of Scientific Research, Princess Nourah bint Abdulrahman University, through the Program of Research Project Funding After Publication, grant No (43-PRFA-P-38).

Data Availability Statement: Not applicable.

Acknowledgments: This research project was funded by the Deanship of Scientific Research, Princess Nourah bint Abdulrahman University, through the Program of Research Project Funding After Publication, grant No (43-PRFA-P-38).

Conflicts of Interest: The authors declare no conflict of interest.

Abbreviation

ACO	Ant colony optimisation
AI	Artificial intelligence
ANN	Artificial neural network
ARMO	Adaptive radial movement optimisation
AOS	Atomic orbital search
BE	Binding energy
BS	Binding state
CSO	Cat swarm optimization
CS-PSO	Cuckoo search-particle swarm Optimisation
FLC	Fuzzy logic control
GA	Genetic algorithm
GSA	Gravitational search algorithm
GTO	Gaussian type orbitals
HHO	Harris hawk optimization
HIL	Hardware-in-the-loop
InC	Incremental conductance
INR	Incremental resistance
JSO	Jellyfish search optimization
LCAO	Linear combination of atomic orbitals
LE)	Leading entity
LMPP	Local maximum power points
MPP	Maximum power point
MPPT	Maximum power point tracking
PDF	Probabilistic density function
P&O	Perturb and observe
PS	Partial shading
PSO	Particle swarm optimisation
PV	Photovoltaic

PWM	Pulse width modulation
SA	Simulated annealing
STC	Standard test conditions
STO	Slater type orbitals
TSA	Tunicate swarm algorithm
TLBO	Teaching learning-based optimisation

References

1. Edenhofer, O.; Madruga, R.P.; Sokona, Y.; Seyboth, K.; Matschoss, P.; Kadner, S.; Zwickel, T.; Eickemeier, P.; Hansen, G.; Schlömer, S.; et al. *Renewable Energy Sources and Climate Change Mitigation: Special Report of the Intergovernmental Panel on Climate Change*; Intergovernmental Panel on Climate Change (IPCC): Geneva, Switzerland, 2011; pp. 1–1075. [CrossRef]
2. Andrei, H.; Dogaru-Ulieru, V.; Chicco, G.; Cepisca, C.; Spertino, F. Photovoltaic Applications. *J. Mater. Process. Technol.* **2007**, *181*, 267–273. [CrossRef]
3. Verma, D.; Nema, S.; Shandilya, A.M.; Dash, S.K. Maximum Power Point Tracking (MPPT) Techniques: Recapitulation in Solar Photovoltaic Systems. *Renew. Sustain. Energy Rev.* **2016**, *54*, 1018–1034. [CrossRef]
4. Salem, F.; Awadallah, M.A. Detection and Assessment of Partial Shading in Photovoltaic Arrays. *J. Electr. Syst. Inf. Technol.* **2016**, *3*, 23–32. [CrossRef]
5. Vieira, R.G.; de Araújo, F.M.U.; Dhimish, M.; Guerra, M.I.S. A Comprehensive Review on Bypass Diode Application on Photovoltaic Modules. *Energies* **2020**, *13*, 2472. [CrossRef]
6. Elgendy, M.A.; Zahawi, B.; Atkinson, D.J. Assessment of the Incremental Conductance Maximum Power Point Tracking Algorithm. *IEEE Trans. Sustain. Energy* **2013**, *4*, 108–117. [CrossRef]
7. Elgendy, M.A.; Zahawi, B.; Atkinson, D.J. Assessment of Perturb and Observe MPPT Algorithm Implementation Techniques for PV Pumping Applications. *IEEE Trans. Sustain. Energy* **2012**, *3*, 21–33. [CrossRef]
8. Guruambeth, R.; Ramabadran, R. Fuzzy Logic Controller for Partial Shaded Photovoltaic Array Fed Modular Multilevel Converter. *IET Power Electron.* **2016**, *9*, 1694–1702. [CrossRef]
9. Elobaid, L.M.; Abdelsalam, A.K.; Zakzouk, E.E. Artificial Neural Network-Based Photovoltaic Maximum Power Point Tracking Techniques: A Survey. *IET Renew. Power Gener.* **2015**, *9*, 1043–1063. [CrossRef]
10. Hussain, M.T.; Sarwar, A.; Tariq, M.; Urooj, S.; BaQais, A.; Hossain, M.A. An Evaluation of ANN Algorithm Performance for MPPT Energy Harvesting in Solar PV Systems. *Sustainability* **2023**, *15*, 11144. [CrossRef]
11. El-Ghajghaj, A.; Karmouni, H.; El Ouanjli, N.; Jamil, M.O.; Qjidaa, H.; Sayyouri, M. Comparative Analysis of Classical and Meta-Heuristic MPPT Algorithms in PV Systems Under Uniform Condition. In *Digital Technologies and Applications, Proceedings of the International Conference on Digital Technologies and Applications, Fez, Morocco, 27–28 January 2023*; Lecture Notes in Networks and Systems; Springer: Berlin/Heidelberg, Germany, 2023; Volume 668, pp. 714–723. [CrossRef]
12. Akyol, S.; Alatas, B. Plant Intelligence Based Metaheuristic Optimization Algorithms. *Artif. Intell. Rev.* **2017**, *47*, 417–462. [CrossRef]
13. Chauhan, S.S.; KumKatoch, S.; Ar, V. A Review on Genetic Algorithm: Past, Present, and Future. *Multimed. Tools Appl.* **2020**, *80*, 8091–8126.
14. Hilali, A.; Mardoude, Y.; Essahlaoui, A.; Rahali, A.; Ouanjli, N. El Migration to Solar Water Pump System: Environmental and Economic Benefits and Their Optimization Using Genetic Algorithm Based MPPT. *Energy Rep.* **2022**, *8*, 10144–10153. [CrossRef]
15. Gad, A.G. Particle Swarm Optimization Algorithm and Its Applications: A Systematic Review. *Arch. Comput. Methods Eng.* **2022**, *29*, 2531–2561. [CrossRef]
16. Li, H.; Yang, D.; Su, W.; Lü, J.; Yu, X. An Overall Distribution Particle Swarm Optimization MPPT Algorithm for Photovoltaic System under Partial Shading. *IEEE Trans. Ind. Electron.* **2019**, *66*, 265–275. [CrossRef]
17. Liu, Y.H.; Huang, S.C.; Huang, J.W.; Liang, W.C. A Particle Swarm Optimization-Based Maximum Power Point Tracking Algorithm for PV Systems Operating under Partially Shaded Conditions. *IEEE Trans. Energy Convers.* **2012**, *27*, 1027–1035. [CrossRef]
18. Alam, A.; Verma, P.; Tariq, M.; Sarwar, A.; Alamri, B.; Zahra, N.; Urooj, S. Jellyfish Search Optimization Algorithm for Mpp Tracking of Pv System. *Sustainability* **2021**, *13*, 11736. [CrossRef]
19. Chou, J.S.; Truong, D.N. A Novel Metaheuristic Optimizer Inspired by Behavior of Jellyfish in Ocean. *Appl. Math. Comput.* **2021**, *389*, 125535. [CrossRef]
20. Zsiborács, H.; Baranyai, N.H.; Vincze, A.; Pintér, G. An Economic Analysis of the Shading Effects of Transmission Lines on Photovoltaic Power Plant Investment Decisions: A Case Study. *Sensors* **2021**, *21*, 4973. [CrossRef] [PubMed]
21. Dorigo, M.; Stützle, T. Ant Colony Optimization: Overview and Recent Advances. *Int. Ser. Oper. Res. Manag. Sci.* **2019**, *272*, 311–351. [CrossRef]
22. Krishnan, G.; Satheesh; Kinattingal, S.; Simon, S.P.; Nayak, P.S.R. MPPT in PV Systems Using Ant Colony Optimisation with Dwindling Population. *IET Renew. Power Gener.* **2020**, *14*, 1105–1112. [CrossRef]
23. Huang, C.; Zhang, Z.; Wang, L.; Song, Z.; Long, H. A Novel Global Maximum Power Point Tracking Method for PV System Using Jaya Algorithm. In Proceedings of the 2017 IEEE Conference on Energy Internet and Energy System Integration (EI2), Beijing, China, 26–28 November 2017. [CrossRef]

24. Pervez, I.; Sarwar, A.; Tayyab, M.; Sarfraz, M. Gravitational Search Algorithm (GSA) Based Maximum Power Point Tracking in a Solar PV Based Generation System. In Proceedings of the 2019 Innovations in Power and Advanced Computing Technologies (i-PACT), Vellore, India, 22–23 March 2019. [CrossRef]
25. Rezk, H.; Fathy, A. Simulation of Global MPPT Based on Teaching–Learning-Based Optimization Technique for Partially Shaded PV System. *Electr. Eng.* **2017**, *99*, 847–859. [CrossRef]
26. Pervez, I.; Sarwar, A.; Pervez, A.; Tariq, M.; Zaid, M. Maximum Power Point Tracking of a Partially Shaded Solar PV Generation System Using Coyote Optimization Algorithm (COA). In *Advances in Electromechanical Technologies, Proceedings of the TEMT 2019, International Conference on Emerging Trends in Electro-Mechanical Technologies and Management, New Delhi, India, 26–27 July 2019*; Lecture Notes in Networks and Systems; Springer: Berlin/Heidelberg, Germany, 2020; pp. 509–518. [CrossRef]
27. Pervez, I.; Sarwar, A.; Pervez, A.; Tariq, M.; Zaid, M. An Improved Maximum Power Point Tracking (MPPT) of a Partially Shaded Solar PV System Using PSO with Constriction Factor (PSO-CF). In *Advances in Electromechanical Technologies, Proceedings of the TEMT 2019, International Conference on Emerging Trends in Electro-Mechanical Technologies and Management, New Delhi, India, 26–27 July 2019*; Lecture Notes in Networks and Systems; Springer: Berlin/Heidelberg, Germany, 2020; pp. 499–507. [CrossRef]
28. Lian, K.L.; Jhang, J.H.; Tian, I.S. A Maximum Power Point Tracking Method Based on Perturb-and-Observe Combined with Particle Swarm Optimization. *IEEE J. Photovolt.* **2014**, *4*, 626–633. [CrossRef]
29. Seyedmahmoudian, M.; Soon, T.K.; Horan, B.; Ghandhari, A.; Mekhilef, S.; Stojcevski, A. New ARMO-Based MPPT Technique to Minimize Tracking Time and Fluctuation at Output of PV Systems under Rapidly Changing Shading Conditions. *IEEE Trans. Ind. Inform.* **2019**. [CrossRef]
30. Badis, A.; Mansouri, M.N.; Sakly, A. PSO and GA-Based Maximum Power Point Tracking for Partially Shaded Photovoltaic Systems. In Proceedings of the 2016 7th International Renewable Energy Congress (IREC), Hammamet, Tunisia, 22–24 March 2016. [CrossRef]
31. Senthilkumar, S.; Mohan, V.; Deepa, R.; Nuthal Srinivasan, M.; Senthil Kumar, T.; Thanikanti, S.B.; Prathap, N. A Review on Mppt Algorithms for Solar Pv Systems. *Int. J. Res.-GRANTHAALAYAH* **2023**, *11*, 25–64. [CrossRef]
32. Thangam, T.; Muthuvel, K. PFoPID CONTROL DESIGN OF GRID-CONNECTED PV INVERTER FOR MPPT USING HYBRID ALGORITHM. *Int. J. Power Energy Syst.* **2022**, *42*, 1–8. [CrossRef]
33. Sharma, A.; Sharma, A.; Jately, V.; Averbukh, M.; Rajput, S.; Azzopardi, B. A Novel TSA-PSO Based Hybrid Algorithm for GMPP Tracking under Partial Shading Conditions. *Energies* **2022**, *15*, 3164. [CrossRef]
34. Kumar, P.; Kumar, M.; Bansal, A.K. GMPP Tracking of Solar PV System Using Spotted Hyena and Quadratic Approximation Based Hybrid Algorithm under Partially Shaded Conditions. *IEEE Access* **2023**. [CrossRef]
35. Hafeez, M.A.; Naeem, A.; Akram, M.; Javed, M.Y.; Asghar, A.B.; Wang, Y. A Novel Hybrid MPPT Technique Based on Harris Hawk Optimization (HHO) and Perturb and Observer (P&O) under Partial and Complex Partial Shading Conditions. *Energies* **2022**, *15*, 5550. [CrossRef]
36. Abo-Khalil, A.G.; El-Sharkawy, I.I.; Radwan, A.; Memon, S. Influence of a Hybrid MPPT Technique, SA-P&O, on PV System Performance under Partial Shading Conditions. *Energies* **2023**, *16*, 577. [CrossRef]
37. Kumar, D.; Chauhan, Y.K.; Pandey, A.S.; Srivastava, A.K.; Kumar, V.; Alsaif, F.; Elavarasan, R.M.; Islam, M.R.; Kannadasan, R.; Alsharif, M.H. A Novel Hybrid MPPT Approach for Solar PV Systems Using Particle-Swarm-Optimization-Trained Machine Learning and Flying Squirrel Search Optimization. *Sustainability* **2023**, *15*, 5575. [CrossRef]
38. Azizi, M. Atomic Orbital Search: A Novel Metaheuristic Algorithm. *Appl. Math. Model.* **2021**, *93*, 657–683. [CrossRef]
39. Hoggan, P.E.; Ruiz, M.B.; Ozdogan, T. Molecular Integrals over Slater-Type Orbitals. From Pioneers to Recent Progress. In *Quantum Frontiers of Atoms and Molecules*; Nova Science Publishers, Inc.: Hauppauge, NY, USA, 2010; pp. 63–90.
40. Azizi, M.; Talatahari, S.; Giaralis, A. Optimization of Engineering Design Problems Using Atomic Orbital Search Algorithm. *IEEE Access* **2021**, *9*, 102497–102519. [CrossRef]
41. Ali, F.; Sarwar, A.; Ilahi Bakhsh, F.; Ahmad, S.; Ali Shah, A.; Ahmed, H. Parameter Extraction of Photovoltaic Models Using Atomic Orbital Search Algorithm on a Decent Basis for Novel Accurate RMSE Calculation. *Energy Convers. Manag.* **2023**, *277*. [CrossRef]